Lasers in Medical Science (2019) 34:1011–1017
https://doi.org/10.1007/s10103-018-2691-6

ORIGINAL ARTICLE

Laryngeal temperature simulations during carbon dioxide laser irradiation delivered by a scanning micromanipulator

Lou Reinisch[1] · C. Gaelyn Garrett[2]

Received: 10 August 2018 / Accepted: 19 November 2018 / Published online: 7 December 2018

Abstract

We use scatter-limited phototherapy techniques to calculate the time-dependent temperature profiles of incisions made with a commercial carbon dioxide laser being used to make a 1-mm incision under computer control using the Digital Acublade™ and with incisions made with the same laser under manual control. The goal is to understand the differences in the amount of lateral thermal damage that is likely from the computer-controlled incisions versus the manually controlled incisions. The temperature profiles are calculated from the absorption and scatter of light in a homogeneous material. The resulting temperature profiles are presented as videos showing how the tissue heats up and cools down with the incident laser pulses. The time-dependent thermal distributions indicate that the computer-controlled laser incision could show as little as 210 μm of lateral thermal damage, whereas the manually controlled laser incisions could show as much as 375 μm of lateral thermal damage. The computer-controlled laser incision is able to control laser pulses fast enough that subsequent pulses can ablate away tissue with a significant amount of residual heat from the previous laser pulse. Using the scatter-limited phototherapy techniques, we can see how a computer-controlled laser can make incisions with less thermal damage by ablating away tissue holding a significant amount of heat from the previous pulse before it has time to diffuse through the tissue. This method of heat removal from laser incisions has not been previously described or demonstrated.

Keywords Carbon dioxide laser · Incision · Computer control · Lateral thermal damage · Scatter-limited phototherapy

Introduction

Laser surgery, especially laser surgery in laryngology, advanced significantly with the invention of the carbon dioxide laser in 1964 by C. Kumar N. Patel [1]. The carbon dioxide laser was the first laser invented with a large absorption coefficient in soft tissue. This allowed the laser to make incisions without a substantial amount of thermal damage to the surrounding tissue. The carbon dioxide laser was also an efficient laser, meaning that minimal water cooling of the laser and sometimes only air cooling was necessary and relatively high output powers were possible. The carbon dioxide laser, due to its large bulky size, was difficult, if not impossible, to use in surgical applications until the invention of the articulated arm by Polanyi in 1967 [2]. Soon after, the addition of the micromanipulator by Bredemeier permitted the laser to be used for many surgical cases in laryngology when the laser was coupled with the surgical microscope [3].

The micromanipulator, articulated arm, and the carbon dioxide laser system underwent a number of improvements and modifications as these instruments became used in more hospitals for an increased number and range of surgical cases. Specifically, the pulse structure of the laser and the spot size of the focused laser beam changed the most. The goal was to more efficiently incise the tissue with less collateral thermal damage, at the same time maintaining the hemostasis of the laser incision.

In the 1990s, we constructed a system where the aiming and scanning of the laser beam was produced with computer-driven mirrors in the micromanipulator [4]. We termed this the CAST system, for computer-assisted surgical techniques. The surgeon could draw the pattern that the laser beam should follow; then,

Electronic supplementary material The online version of this article (https://doi.org/10.1007/s10103-018-2691-6) contains supplementary material, which is available to authorized users.

✉ Lou Reinisch
lou.reinisch@nyit.edu

[1] Academic Affairs, New York Institute of Technology, 1855 Broadway, Manhattan, NY 10023, USA

[2] Department. of Otolaryngology, Vanderbilt University Medical Center, 1215 21st Ave S., Nashville, TN 37232, USA

the computer made certain that the pattern was carefully traced and rapidly repeating laser pulses were spread across the incision pattern to reduce thermal buildup in the tissue. The system was widely used with experimental surgery and was a standard delivery tool for the Vanderbilt free-electron laser. The speed of the computer in directing the laser beam allowed for significant reductions in the lateral thermal damage when making an incision.

The computer-controlled micromanipulator was finally commercially available with the Luminis Digital Acublade™ in 2008 [5]. While the Digital Acublade is a remarkable advancement in laser surgery, it is felt that the advantages of allowing the computer to quickly direct the laser beam have not been fully appreciated.

Brochures for the Digital Acublade tout the ease of use and the increased precision and minimizing the damage to adjacent healthy tissue. The brochures also point out that the rapid scanning movement reduces the procedure time. Our experience from using CAST is that the rapid motion of the laser beam is far more beneficial than simply providing reduced procedure time. The rapid motion of the laser beam can actually reduce the lateral thermal damage. This reduction of thermal damage is similar to the "thermal confinement" from short-pulsed lasers reducing thermal damage. While the fast motion does not change the pulse duration of the laser, it does decrease the "dwell time" that the laser is incident on a specific volume of tissue, thus giving a short pulse effect to the laser incident on a specific volume of tissue.

Independently, we have been working on numerical methods to calculate the tissue temperature while it is undergoing laser irradiation [6–8]. These scatter-limited phototherapy simulations can provide spatial-temporal temperature profiles in tissue during and after laser irradiation. The simulations are made assuming the tissue is homogeneous or comprises large sections of homogeneous tissue. Then, standard scatter and absorption patterns of the light can be calculated given the geometry and the pulse structure of the incoming beam. The light energy is then transformed into a temperature profile given the heat capacity of the tissue and that thermal energy then undergoes thermal diffusion. The exact details of the calculations can be found in Reinisch et al. [7].

The scatter-limited phototherapy model uses independently measured tissue parameters for absorption, scatter, thermal conductivity, and heat capacity to make the calculations. By recognizing that it is well-known and well-understood how light scatters in homogeneous tissue [6–8], we can avoid having to solve inhomogeneous partial differential equations. Thus, the profiles can be rapidly generated, and the profiles as a function of time can be sequenced to create videos. The videos demonstrate the changing thermal gradients inside the tissue during a laser procedure.

We can use the numerical calculations of the temperature profile in tissue to see how a computer-controlled laser incision is different from a highly skilled manual application of the laser to make a similar incision.

Materials and methods

The details of the scatter-limited phototherapy model have been described in detail in previous publications [6–8]. We chose to use this model because the speed of the calculations allows us to make a time series of evaluations. Time-dependent temperature profiles of tissue during and after laser irradiation are extremely valuable in understanding laser therapy.

Since the model uses only measured parameters, it is not a surprise that the calculations of thermal damage from the model agree with the actual measurements of thermal damage. We have shown this correlation between measured thermal damage and the calculations in the near infrared at 1064 nm [6] and in the infrared at 10.6 μm and in the visible at 532 nm [7].

Here we allow *I(x,y,z)* to be the three-dimensional distribution of light in the tissue. z is the coordinate axis into the thickness of the tissue; x and y are orthogonal cross directions. I_0 is the incident intensity of light. In addition to the scatter represented by the reduced scattering coefficient, μ_s, Beer's Law is used to describe the absorption in an isotropic three-dimensional model where μ_a is the absorption coefficient. The light distribution in a homogeneous absorbing and scattering medium can be written as:

$$I(x,y,z) = I_0 \frac{(\mu_s + \mu_a)^3}{4\pi} \exp\left[-(\mu_s + \mu_a)\sqrt{x^2 + y^2 + z^2}\right] \tag{1}$$

Note that scattering and absorption behave much the same way; both scattering and absorption act together to limit the penetration of light. Using Eq. (1) to describe the spread of the light, one does not need to use a Monte Carlo simulation and the calculations take much less computational time than a Monte Carlo simulation.

The absorption of light by water is well understood and the absorption coefficients as a function of wavelength can be obtained from the publication by Hale and Querry [9]. Using a quadratic interpolation between 10.0 and 11.00 μm, results in an absorption coefficient of 797 cm^{-1} for water at 10.6 μm. The absorption of infrared light at 10.6 μm by oxyhemoglobin (HbO_2) and deoxyhemoglobin (Hb) can be ignored. Not only does the protein structure have an extremely weak infrared absorption compared to water, but the mucosa as normal soft tissue with about 75% water [10] and blood is a much smaller component of mucosa. Thus, we use only 75% of water to as the absorption coefficient for the simulations ($\mu_a = 598\ cm^{-1}$).

After we calculate how the light is distributed in the tissue, we then converted that light energy into a temperature increase using the heat capacity of soft tissue, 3.7 J/g°K [7]. The thermal energy is not fixed into the tissue, but it will dissipate or thermally diffuse. The thermal diffusion is modeled with:

$$T(x,y,z,t) = T_{\max} \frac{1}{(4\pi Dt)^{3/2}} Exp\left[-\frac{(x^2 + y^2 + z^2)}{4Dt}\right] \tag{2}$$

In Eq. (2), T is temperature, t is time, and D is the thermal diffusion coefficient. T_{max} is the maximum temperature of the tissue. We can write $D = \kappa/\rho c_p$, where is κ the thermal conductivity of the tissue, ρ is the density of the tissue, and c_p is the specific heat capacity of the tissue. This allows us to independently calculate D for a well-known substance, like water ($D_{water} = 0.0014$ cm^2/s). In these simulations, we use $D_{mucosa} = 0.0023$ cm^2/s for the mucosa. This comes from measurements of thermal damage as a function of laser pulse length [6, 11] and is close to the value of water, as one might expect.

To create the videos, we simply generate temperature profiles with a consistent step in time. The many profiles are then displayed one after the next, creating the videos that are displayed in this publication.

The simulation videos are presented with a consistent time clock, but that time clock changes with the repetition rate of the laser. For instance, the simulation presented here of the Digital Acublade shows contours directly after the incident laser pulse and then at 700 μs steps. Since the laser pulses once every 3.5 ms, the laser pulse arrives once every five frames. The resulting video runs much slower (more than 1000×) than the actual incision time. Recall that the Digital Acublade makes the incision in 35 ms and the video of the 11 laser pulses runs for about 45 s. The slo-mo effect of the videos helps to visualize how the heat spreads during the incision. The laser pulse length and repetition rate used in our calculations are the same values that one of the coauthors [CGG] uses in the clinical setting.

The manually controlled laser pulses at a rate that is ten times slower than the Digital Acublade controlled laser pulse. If we kept time steps of 700 μs per frame as we used with the Digital Acublade, it would take 7.5 min of video time to view the manual incision simulation. Instead, we speed up the simulation a factor of ten with 7 ms time steps for each frame. Again, the laser pulses once every five frames. Both the Digital Acublade (video 1) and the uniform step size with a manually controlled laser (video 2) move the beam a distance of 0.075 mm between pulses in a straight line. The second manual simulation (video 3) uses the same slower time (35 ms) to move the laser beam. However, the length of the steps is not uniform. Our experience is when the laser is under manual control, the motion starts out slow (the distance between pulses is very small) and then moves very fast (a large distance between pulses) finally slows down before it the end of the incision (again, small distances between the pulses). So, instead of having the uniform step size of 0.075 mm, the steps are 0.01 mm, 0.02 mm, 0.05 mm, 0.1 mm, 0.2 mm, 0.19 mm, 0.1 mm, 0.05 mm, 0.02 mm, and 0.01 mm in length. We feel this a very good simulation of a very skilled operator manually controlling the laser as it makes the 1-mm incision.

Figure 1 shows the spot patterns for all three simulations. Figure 1a is the Digital Acublade and the manual evenly spaced spot pattern. Figure 1b is the manual unevenly spaced pulses.

The calculated thermal contours are then overlaid on a histology slide of the vocal fold. The highly magnified image shows a 1-mm-long scale bar. The histology slide shows the *vocalis* muscle towards the bottom of the histological slice and the *lamina propria* across the upper portion. Each color change of the calculated thermal contours is a 5 °C greater increase of the ambient temperature caused by the laser light. Thus, it is the tissue that displays aqua or blue that is heated above 60 °C and can contain denatured proteins. Tissues displaying the magenta color have reached 88–100 °C, but not enough energy has been deposited to provide the latent heat of vaporization of water. Thus, the tissue is not ablated.

Even though the tissue might reach 100 °C, it does not necessarily ablate or vaporize. To change the water from liquid water to steam, the latent heat of vaporization must be added to the target in addition to enough heat to bring the temperature up to 100 °C. So, in our simulation, the heat capacity is 3.7 J/g°K. We have to heat the tissue from 37 to 100 °C. This is a 63 °C increase in temperature or 233 J/g of heat is needed to raise the temperature to 100 °C (using 3.7 J/g°K as the heat capacity). We then need to add the latent heat of vaporization (2260 J/g for water or about 1700 J/g for our tissue that is 75% water). Thus, it requires roughly 1933 J/g (233 J/g + 1700 J/g) before the tissue is ablated and removed from the simulation.

The simulations are made with 100-μs laser pulses repeating every 3.5 ms and the laser set to 7 W. These are the clinical settings that are used by the author [CGG]. Seven watts with pulses every 3.5 ms is equivalent to 24.5 mJ per pulse (24.5 mJ/3.5 ms = 7 W). When we slow down the repetition rate to one pulse every 35 ms, instead of 3.5 ms, we should increase the energy per pulse by a factor of ten to keep the same average power (7 W). Instead, we maintain a constant energy per pulse (24.5 mJ) to make equal comparisons. We refer to these slower

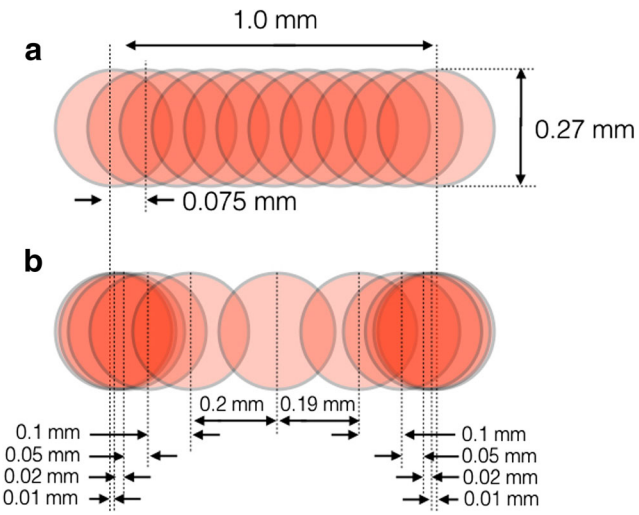

Fig. 1 Graphic representation of the laser spot pattern. **a** Uniformly spaced spots.**b** Unevenly spaced spots. In both cases, 11 pulses are used; the laser is focused to 0.27-mm spot size and the resulting incision is 1 mm long

rep rates as maintaining 7 W, whereas we are actually maintaining a constant energy (number of mJ) per pulse.

Results

The three simulations are shown as visualizations (video files) that can be accessed by computer or smart phone. We give both the URL that can be linked to, manually put into a web browser, or a QR code that can be read with a smart phone or tablet to display the videos.

Visualization #1: the Digital Acublade

For this first simulation, we incident a laser pulse that is about 100 μs long on the tissue and calculate the absorption, scatter, and temperature increase. The tissue that is heated to 100 °C and provided with enough energy to reach the latent heat of vaporization is ablated away. The laser is set to 7 W and focused to 0.27-mm spot size. The laser pulses at one pulse every 3.5 ms. A total of 11 pulses create the 1-mm-long incision with each pulse displaced by 0.075 mm. The laser wavelength is 10.6 μm and the absorption is 75% water or 598 cm^{-1}. Tissue that displays an aqua or blue is heated above 60 °C and can contain denatured proteins. Tissues displaying the magenta color have reached 88 to 100 °C, but not enough energy has been deposited to provide the latent heat of vaporization of water.

Visualization #1: A video simulation of the temperature increase of a vocal fold with an incision made by the Digital Acublade laser. The laser intensity is set to 7 W and a 1-mm-long straight line incision is made will 11 equally spaced pulses delivered in 35 ms. (Click on the URL: https://youtu.be/AbnoUATZYpM to see the video run.)

https://youtu.be/AbnoUATZYpM

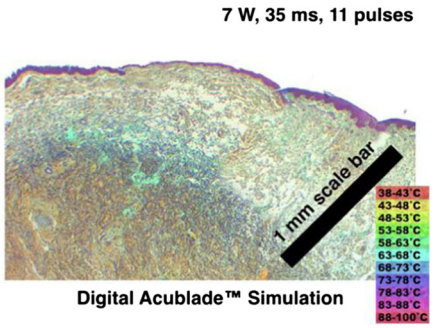

Visualization #2: even step size manual control

For the second simulation, we keep all the parameters the same, except the laser now pulses at one pulse per 35 ms (ten times slower than the simulations in visualization #1, or with the Digital Acublade).

Visualization #2: A video simulation of the temperature increase of a vocal fold with an incision made manually with an even step size. The laser intensity is set to 7 W and a 1-mm-long straight line incision is made will 11 equally spaced pulses delivered in 350 ms. (Click on the URL: https://youtu.be/qGCUnypAsW8 to see the video run.)

https://youtu.be/qGCUnypAsW8

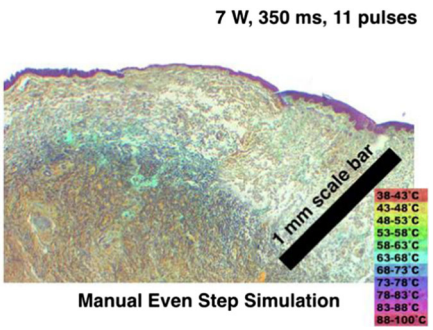

Visualization #3: Realistic step size manual control

Our work with the laser pulses finds that a manually controlled fast incision shows a slow start to the laser scan, an over-compensating scan that is too fast followed by a slow finish. Manually, the scan of the laser beam has an acceleration and deceleration time. Our hands and brains are not able to instantaneously bring the scan to the correct speed and maintain that speed. Thus, this third simulation is probably the most realistic manual simulation to compare to the Digital Acublade. For the third simulation, we use all the same parameters of visualization #2, including the slower repetition rate. However, we replaced the uniform step size of the laser beam (Fig. 1a) by the pattern shown in Fig. 1b. A total of 11 pulses create the 1-mm-long incision with each pulse displaced by 0.01 mm, 0.02 mm, 0.05 mm, 0.1 mm, 0.2 mm, 0.19 mm, 0.1 mm, 0.05 mm, 0.02 mm, and 0.01 mm.

Visualization #3: A video simulation of the temperature increase of a vocal fold with an incision made manually with an uneven step size. The laser intensity is set to 7 W and a 1-mm-long straight line incision is made will 11 pulses, with each pulse displaced by 0.01 mm, 0.02 mm, 0.05 mm, 0.1 mm, 0.14 mm, 0.19 mm, 0.14 mm, 0.1 mm, 0.05 mm, and 0.02 mm, and delivered in 350 ms. (Click on the URL: https://youtu.be/1Pb_tVqMq2M to see the video run.)

https://youtu.be/1Pb_tVqMq2M

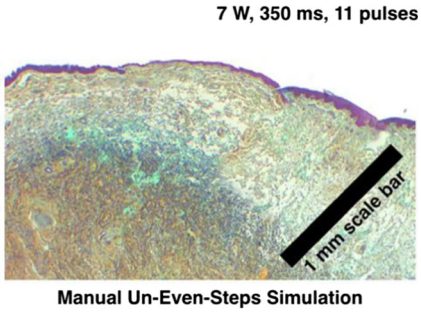

Since collagen and proteins denature at about 60 °C, we show in Fig. 2 the area of the vocal fold that reaches a temperature exceeding 60 °C at some point during the incision and cool-down process. In Fig. 2a, we show the Digital Acublade incision. The zone where the temperature exceeded 60 °C is shown with a darker tint. This zone is relatively uniform and 210 μm wide. In Fig. 2b, we show the equal step size with ten times slower incision. Here, the zone of tissue exceeding 60 °C builds up as the incision is made and the temperature of the tissue increases. The maximum depth for this zone is 375 μm. In Fig. 2c, we show the unequal step size with the ten times slow incision, or our simulation of a skilled manual incision. Here, the zone of tissue exceeding 60 °C is variable with the maximum depth of 375 μm.

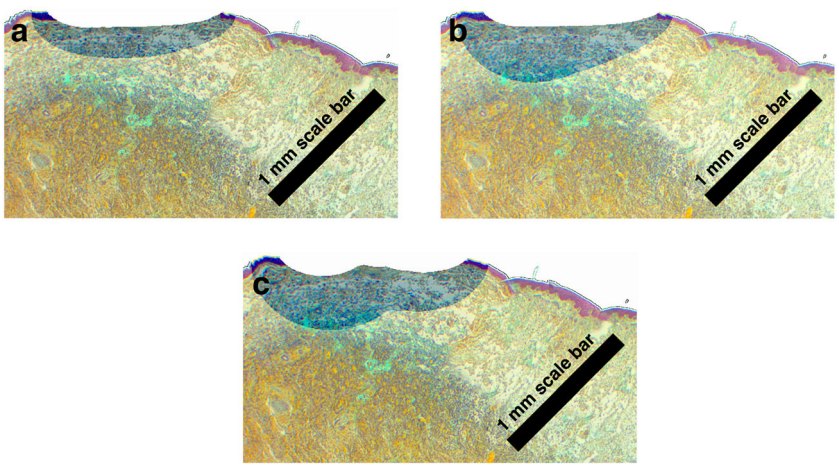

Fig. 2 Zone of tissue exceeding 60 °C is shown as a darker tint overlaying the vocal fold histology. **a** Shows the Digital Acublade with a nearly uniform 210-μm-wide zone. **b** Shows the equal step size with ten times slower laser repetition rate. The maximum zone thickness is 375 μm. **c** Shows the unequal step size with ten times slower laser repetition rate. The maximum zone thickness is 375 μm. All the laser parameters are the same as the three simulations shown above

Discussion

We have compared temperature profiles from the Digital Acublade used with the parameters that can be used in laryngeal surgery to temperature profiles from simulations that approximate manual incisions. When making the transition from the Digital Acublade to the manual incisions, we first slowed the process so that it takes 350 ms to make the 1-mm-long incision instead of the 35 ms that the Digital Acublade requires. We then used both the slow incision time (350 ms) with uneven step sizes (see Fig. 1b) to best simulate a manually produced incision by a skilled operator. Both the slower repetition rate and the uneven step size cause more collateral thermal damage than is seen with the Digital Acublade (see Fig. 2).

What is shown in these simulations and the resulting videos (see Videos 1–3) is the reason that the Digital Acublade creates a reduced amount of lateral thermal damage. We note that the lateral thermal damage from a carbon dioxide laser incision is normally given to be in the range of 300 to 350 μm [12]. Here, we see less thermal damage when using the Digital Acublade and approximately the same amount or perhaps a bit more thermal with the slower scanned laser beam from the simulations of a manually controlled beam.

In the simulations, each laser pulse ablates tissue and leaves a perimeter of tissue that is heated to 100 °C, but lacks enough heat to vaporize the water. In the video, this tissue is colored magenta. This zone of water at 100 °C with excess heat spreads relatively quickly to the adjacent tissue. The magenta area spreads out in the video. As with the Digital Acublade, when the subsequent laser pulse comes to a mere 3.5 ms later, the collateral heat has not spread very far. Therefore, the next laser pulse is able to ablate away a significant portion of this heated tissue. The ablation of the heated tissue removes some of the collateral heat from the remaining tissue. This way each laser pulse removes a significant amount of the heat left in the tissue from the previous pulse. This heat removal by the rapidly following next pulse is what causes the incision to show zones heated in excess of 60 °C that are only 210 μm deep.

On the other hand, when the subsequent laser pulse comes 35 ms after the first pulse, as we simulate for a manually controlled incision, the heat from the very hot magenta-colored tissue has had enough time to spread through a relatively large volume of the tissue. So, the second laser pulse does not ablate away a significant amount of the extremely hot tissue. That heat has already spread far beyond the range of the subsequent ablation crater. In this way, each laser pulse leaves most of the energy from the previous pulse and adds even more thermal energy into the tissue. This buildup of heat in the tissue results in zones that are 375 μm deep where the temperature of the adjacent tissue exceeds 60 °C.

The fact that the Digital Acublade can make the entire 1-mm incision with 11 laser pulses in 35 ms is the key aspect that actually reduces the lateral thermal damage of the carbon dioxide surgical laser. We can compare this to the condition when the pulses come at a slower rate, and it takes 350 ms to make the 1-mm incision, the collateral heat from the preceding laser pulse has had enough time to spread into a large volume of tissue. This builds up heat in the tissue and increases the amount of lateral tissue damage. The human hand is not able to precisely move the laser beam with only 3.5 ms between the laser pulses. It is only when using a mechanically scanned laser beam that the reduced lateral thermal tissue damage can be realized when making a laser incision.

We can also see that the increased time between the laser pulses leads to the buildup of heat in the tissue. This is more significant than the uneven step size when not using the mechanical scanner. While various publications mention the speed at which the Digital Acublade makes an incision, clinically it is not important if the incision is made in 35 ms or 350 ms. Both incisions are made in less than 1 s. However, the speed is extremely important to the amount of heat in the tissue. We are not aware of any previous publication coupling the speed of the incision process with the amount of heat removed from the tissue with subsequent laser pulses. In terms of heat removal, the difference between 35 and 350 ms is significantly important.

We note some other interesting information that we gathered from this series of simulations. The first is that the laser pulse delivers 24.5 mJ of energy to the tissue. Most of that energy is used to ablate the tissue. After the laser pulse, there is about 6 mJ of heat energy, in total, left in the tissue. Or, we might state that the laser is 75% efficient in removing tissue. Seventy-five percent of the energy of the laser pulse is ablated away. One might ask how this efficiency might be increased with a change in the pulse energy or a change in the size of the focused laser beam?

We also note that there is a measurable spread of the thermal profile during the 3.5 ms. How much could the lateral thermal damage be further reduced by engineering a carbon dioxide laser with an even faster repetition rate for the pulses?

We find these simulations and the videos generated of the time-dependent temperature profiles to be instructive and enlightening. We strongly believe that this information can help us to design even better laser delivery systems and to understand the laser delivery systems that we are currently using.

Conclusion

The simulations of the Digital Acublade with a carbon dioxide laser with settings for laryngeal surgery show the potential for less lateral thermal damage than a manually controlled laser. The reduction of thermal damage is largely due to the extremely short time (3.5 ms) between pulses with the Digital Acublade. This short time does not allow the residual heat from the previous laser pulse to spread very far. The subsequent laser pulse then ablates away tissue that contains a

significant amount of that residual heat, thus reducing the overall amount of heat in the tissue. The scatter-limited phototherapy model is shown to be helpful in understanding laser-tissue interactions.

Compliance with ethical standards This article does not contain any studies with human participants or animals performed by any of the authors.

Conflict of interest The authors declare that they have no conflict of interest.

References

1. Patel CKN (1964) Continuous-wave laser action on vibrational-rotational transitions of CO_2. Phys Rev 136(5A):A1187–A1193
2. Polanyi TG, Bredemeier HC, Davis TW Jr (1970) A CO_2 laser for surgical research. Med Biol Eng 8(6):541–548
3. Bredemeier H (1974) "Stereo laser endoscope," US Patent 3796220 A. United States patent and trademark office, USPTO patent full-text and image database patft.uspto.gov/netacgi/nph-Parser?Sect2=PTO1&Sect2=HITOFF&p=1&u=/netahtml/PTO/searchsearchbool.html&r=1&f=G&l=50&d=PALL&RefSrch=yes&Query=PN/3796220
4. Reinisch L, Mendenhall M, Charous S, Ossoff RH (1994) Computer assisted surgical techniques utilizing the Vanderbilt free electron laser. Laryngoscope 104:1323-1329
5. Remacle M, Lawson G, Nollevaux MC, Delos M (2008) Current state of scanning micromanipulator applications with the carbon dioxide laser. Ann Otol Rhinol Laryngol 117(4):239–244
6. Reinisch L (2002) Scatter-limited phototherapy: a model for laser treatment of skin. Lasers Surg Med 30:381–388
7. Reinisch L, Garrett CG, Courey M (2013) A simplified laser treatment planning system: proof of concept. Lasers Surg Med 45:679–685
8. Harris DM, Reinisch L (2016) Selective Photoantisepsis. Lasers Surg Med 48:763–773
9. Hale GM, Querry MR (1973) Optical constants of water in the 200 nm to 200 μm wavelength region. Appl Opt 12(3):555–563
10. Forbes RM, Cooper AR, Mitchell HH (1953) The composition of the adult human body as determined by chemical analysis. J Biol Chem 203:359–366
11. Valvano JW, Cochran JR, Diller KR (1985) Thermal conductivity and diffusivity of biomaterials measured with self-heating thermistors. Int J Thermophys 6:301–311
12. Sanders DL, Reinisch L (2000) Wound healing and collagen thermal damage in 7.5-μsec pulsed CO_2 laser skin incisions. Laser Surg Med 26:22–32